Neuron
Article

GlialCAM, a Protein Defective in a Leukodystrophy, Serves as a ClC-2 Cl^- Channel Auxiliary Subunit

Elena Jeworutzki,[1,11] Tania López-Hernández,[2,11] Xavier Capdevila-Nortes,[2] Sònia Sirisi,[2,5] Luiza Bengtsson,[4] Marisol Montolio,[2,6] Giovanni Zifarelli,[1] Tanit Arnedo,[2] Catrin S. Müller,[8] Uwe Schulte,[8] Virginia Nunes,[3,5,7] Albert Martínez,[9] Thomas J. Jentsch,[4] Xavier Gasull,[10] Michael Pusch,[1,11] and Raúl Estévez[2,6,11,*]
[1]Istituto di Biofisica, Consiglio Nazionale delle Ricerche, 16149 Genoa, Italy
[2]Physiology section
[3]Genetic section
Department Physiological Sciences II, School of Medicine, University of Barcelona, 08907 Barcelona, Spain
[4]Leibniz-Institut für Molekulare Pharmakologie (FMP) and Max-Delbrück-Centrum für Molekulare Medizin (MDC), D-13125 Berlin, Germany
[5]Laboratorio de Genética Molecular-IDIBELL
[6]U-750, Centro de Investigación en Red de Enfermedades Raras (CIBERER), ISCIII
[7]U-730, Centro de Investigación en Red de Enfermedades Raras (CIBERER), ISCIII
[8]Logopharm GmbH, D-79232 March-Buchheim, Germany
[9]Department of Cell Biology, Faculty of Biology, University of Barcelona, 08028 Barcelona, Spain
[10]Laboratory Neurophysiology, Department Physiological Sciences I, School of Medicine, University of Barcelona-IDIBAPS, 08007, Spain
[11]These authors contributed equally to this work
*Correspondence: restevez@ub.edu
DOI 10.1016/j.neuron.2011.12.039

SUMMARY

Ion fluxes mediated by glial cells are required for several physiological processes such as fluid homeostasis or the maintenance of low extracellular potassium during high neuronal activity. In mice, the disruption of the Cl^- channel ClC-2 causes fluid accumulation leading to myelin vacuolation. A similar vacuolation phenotype is detected in humans affected with megalencephalic leukoencephalopathy with subcortical cysts (MLC), a leukodystrophy which is caused by mutations in *MLC1* or *GLIALCAM*. We here identify GlialCAM as a ClC-2 binding partner. GlialCAM and ClC-2 colocalize in Bergmann glia, in astrocyte-astrocyte junctions at astrocytic endfeet around blood vessels, and in myelinated fiber tracts. GlialCAM targets ClC-2 to cell junctions, increases ClC-2 mediated currents, and changes its functional properties. Disease-causing *GLIALCAM* mutations abolish the targeting of the channel to cell junctions. This work describes the first auxiliary subunit of ClC-2 and suggests that ClC-2 may play a role in the pathology of MLC disease.

INTRODUCTION

Megalencephalic leukoencephalopathy with subcortical cysts (MLC) is a rare type of leukodystrophy (van der Knaap et al., 1995a) characterized by macrocephaly that appears in the first years of life. MRI of patients shows swelling of the cerebral white matter and the presence of subcortical cysts, mainly in the anterior temporal regions. In MLC patients, diffusion studies indicate increased water content of the brain (van der Knaap et al., 1995b). A brain biopsy from an MLC patient revealed myelin (van der Knaap et al., 1996) and astrocyte vacuolation (Duarri et al., 2011). It was suggested that MLC may be caused by impaired ion transport across cellular membranes, thereby leading to an osmotic imbalance and disturbed fluid homeostasis (Brignone et al., 2011; Duarri et al., 2011). Indeed, *MLC1*, the first disease gene discovered to underlie MLC in most patients (Leegwater et al., 2001), encodes an integral membrane protein with 8 putative transmembrane domains with low and questionable homology to ion channels (Teijido et al., 2004). Recently, MLC1 has been proposed to be related to the activation of the volume-regulated anion channel (Ridder et al., 2011). However, the precise role of MLC1 in volume-regulated chloride transport is not clear (Ridder et al., 2011).

Among the ion channels that are expressed in glia, the hyperpolarization-activated and osmosensitive ClC-2 Cl^- channel (Gründer et al., 1992; Thiemann et al., 1992) has been proposed to be an important player in extracellular ion homeostasis (Blanz et al., 2007; Fava et al., 2001; Makara et al., 2003). Mice lacking ClC-2 (*Clcn2*$^{-/-}$ mice) exhibit vacuolation of the white matter that resembles the pathology of MLC patients (Blanz et al., 2007). *MLC1* mutations account for only 75% of patients with MLC, but none of the patients without mutations in *MLC1* carried bona fide disease-causing mutations in *CLCN2* (Blanz et al., 2007; Scheper et al., 2010). Tests for a crosstalk between ClC-2 and MLC1 also gave negative results. The proteins could not be coprecipitated, and reduction of MLC1 levels by RNA interference did not change ClC-2 protein levels (Duarri et al., 2011). Hence, no role of ClC-2 in human MLC could be established.

GLIALCAM was recently identified as a second MLC gene (López-Hernández et al., 2011a). GlialCAM is an Ig-like cell-adhesion molecule of poorly characterized function (Favre-Kontula

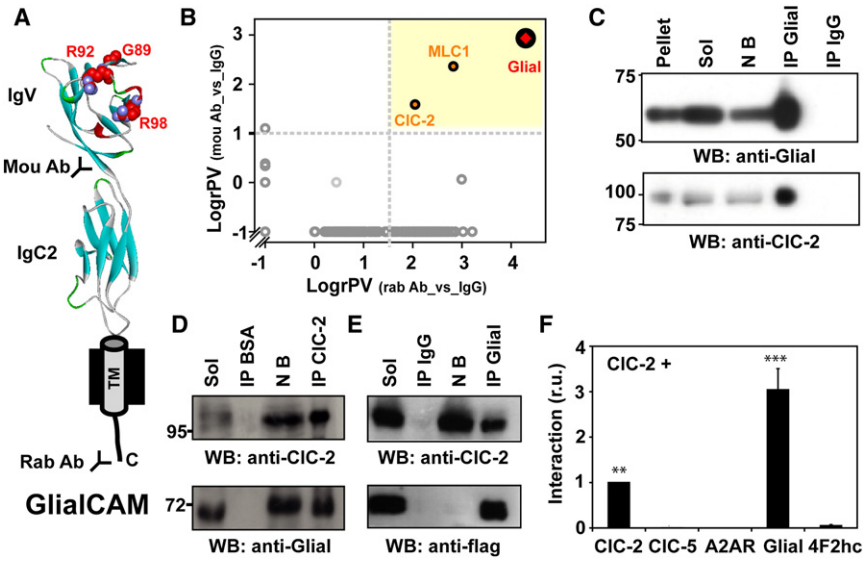

Figure 1. Identification of ClC-2 as a GlialCAM-Interacting Protein

(A) Scheme of the GlialCAM molecule. Mutated residues studied in this work are depicted. Antibodies used for purification (mou: mouse; rab: rabbit) are shown.

(B) Evaluation of GlialCAM affinity purification from mouse brain. The scheme shows a 2D plot of relative protein enrichment in affinity purifications versus IgG controls. Proteins specifically copurified are shown in the yellow area; dashed lines indicate the specificity thresholds as suggested by the distribution of all protein ratios (gray circles).

(C), Immunoblot analysis of a sample of the affinity purification with the anti-GlialCAM rabbit polyclonal antibody stained with the same antibody (upper) and with anti-ClC-2 C1 antibody (lower); lanes resolve aliquots of pellet after solubilization, solubilizate (Sol), not bound (NB), or eluates from the purification (IP Glial). IP IgG: eluate from an IgG control.

(D) Copurification of GlialCAM with anti-ClC-2 C2 antibody. Lanes were labeled as before.

(E) Coimmunoprecipitation from HeLa cells transiently transfected with ClC-2 and Flag-tagged GlialCAM. Lanes were labeled as before.

(F) Quantification of interaction using the split-TEV assay. ClC-2 was tested for interaction with the proteins indicated below the graph. $^{**}p < 0.01$; $^{***}p < 0.001$ versus 4F2hc.

See also Figure S1.

et al., 2008). A role of GlialCAM in MLC was first suggested by biochemical assays that demonstrated that both proteins bind each other and colocalize in astrocyte-astrocyte junctions at astrocytic endfeet (López-Hernández et al., 2011a). GlialCAM targets MLC1 to cell-cell junctions (López-Hernández et al., 2011b) and *GLIALCAM* mutations identified in MLC patients impair the correct trafficking of GlialCAM and MLC1 to astrocyte-astrocyte junctions (López-Hernández et al., 2011a, 2011b).

Unlike MLC1, GlialCAM is also detected in myelin (López-Hernández et al., 2011a), mainly in oligodendroglial extensions (Favre-Kontula et al., 2008). In the present work, we show that GlialCAM interacts with ClC-2 in several glial cell types including oligodendrocytes, targeting it to cell junctions and dramatically increasing its conductance. We thus identified GlialCAM as an auxiliary subunit of ClC-2, potentially implicating the channel in the pathogenesis of MLC.

RESULTS

Identification of ClC-2 as GlialCAM Binding Partner

We used two different antibodies directed against GlialCAM (Figure 1A) to identify proteins from solubilized mouse brain membranes that copurify with GlialCAM. In addition to peptides from GlialCAM and MLC1, quantitative mass spectroscopy identified peptides corresponding to the ClC-2 chloride channel (Figure 1B and see Figure S1 available online) as the only other consistently and specifically copurified protein in the eluate. Western blot analysis confirmed that ClC-2 was copurified with at least a fraction of GlialCAM (Figure 1C), which may result from a partial dissociation of the complex or may indicate that not all GlialCAM is associated with ClC-2. Coimmunoprecipitation experiments using an antibody against ClC-2 confirmed the interaction between GlialCAM and ClC-2 (Figure 1D). Similar experiments using extracts from cells transfected with ClC-2 and C terminally tagged GlialCAM (Figure 1E), as well as split-TEV interaction experiments (Figure 1F), suggested that ClC-2 and GlialCAM directly interact. The interaction appeared specific since no association was observed between ClC-2 and the related $2Cl^-/H^+$ antiporter ClC-5, the unrelated polytopic adenosine 2A receptor (A2AR), or the unrelated single transmembrane span protein 4F2hc (Figure 1F).

Colocalization of ClC-2 and GlialCAM in Tissue

For the interaction of GlialCAM and ClC-2 to be physiologically relevant, both proteins must colocalize in native tissue. GlialCAM is found exclusively in brain, where it localizes to astrocyte-astrocyte junctions at endfeet, Bergmann glia, some pyramidal neurons and to myelin (López-Hernández et al., 2011a). In addition to neurons, ClC-2 is expressed on astrocytes and oligodendrocytes and was found in myelin-enriched fractions (Blanz et al., 2007; Fava et al., 2001; Földy et al., 2010; Makara et al., 2003; Rinke et al., 2010; Sík et al., 2000). GlialCAM colocalized in mouse brain with ClC-2 in cerebellar Bergmann glia which was counterstained for GFAP (Figure 2A). Both proteins were present at astrocytic endfeet surrounding blood vessels (Figure 2B; Blanz et al., 2007; López-Hernández et al., 2011a; Sík et al., 2000) in the cortex and in the cerebellum. In human cerebellum, immunogold electron microscopy detected ClC-2 at astrocyte-astrocyte contacts in the endfeet (Figures 2C and 2D), a location where also GlialCAM and MLC1 are present (López-Hernández et al., 2011a). GlialCAM and ClC-2 were also found to colocalize in myelinated fiber tracts along the circumference of oligodendrocytic cell bodies in mouse cerebellum (Figure 2E), where GlialCAM, ClC-2, and the oligodendrocyte-expressed gap junction protein Cx47 were present in the same cell membrane (Figure 2F; Blanz et al., 2007). In vitro cell culture

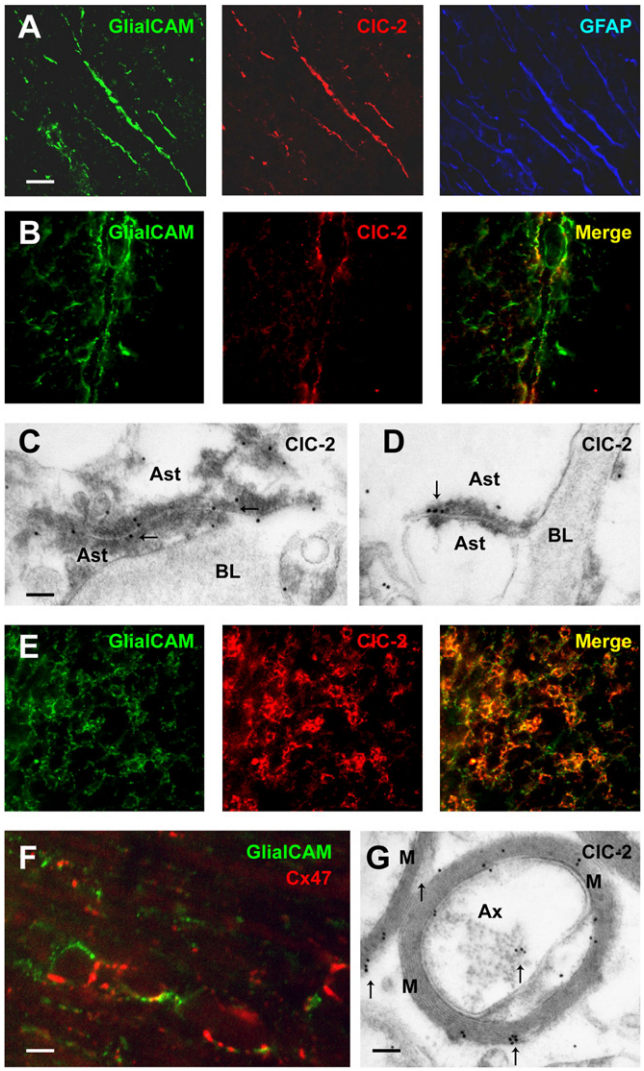

Figure 2. Localization of ClC-2 and GlialCAM in the Brain

Mouse brain sections labeled with antibodies against GlialCAM, ClC-2, or GFAP antibodies. (A) cerebellar Bergmann glia; (B) astrocytic endfeet surrounding blood vessels in cortex; (C and D) EM immunolabeling of human cerebellum shows localization of ClC-2 (arrows) in astrocyte-astrocyte junctions near basal lamina; (E) oligodendrocytic cell bodies in myelinated fibers of cerebellar white matter tracts.

(F) Coexpression of GlialCAM and the oligodendrocyte marker Cx47 in membranes of oligodendrocytic bodies in the cerebellum.

(G) EM immunolabeling detects ClC-2 in myelin (arrows).

Scale bars for (A), (B), and (E) 20 μm; (F) 5 μm; for panels (C) and (D) 200 nm; (G) 500 nm. M: myelin; Ax: axon; Ast: astrocyte; BL: basal lamina. ClC-2 antibodies used: C1 (A); C2 (B–F). See also Figure S2.

studies have shown that GlialCAM is expressed in different stages of oligodendrocytic differentiation, including the bipotential O2-A progenitor NG2 positive cells (OPC cells) (Favre-Kontula et al., 2008). Immunogold EM confirmed the presence of ClC-2 in human myelin (Figure 2G).

Localization and expression of GlialCAM is independent of MLC1 (López-Hernández et al., 2011b). We similarly asked whether the expression of GlialCAM or MLC1 depends on ClC-2. Western blots revealed that the total amount of GlialCAM and MLC1 proteins were unchanged in the brain of *Clcn2*$^{-/-}$ mice (Figure S2A). Likewise, there was no change in the subcellular localization of GlialCAM and MLC1 in Bergmann glia, nor in the astrocytic endfeet around blood vessels in *Clcn2*$^{-/-}$ mice (Figures S2B and S2C).

GlialCAM Changes the Subcellular Distribution of ClC-2

We then studied whether GlialCAM changes the abundance or localization of ClC-2 in heterologous expression systems. We could not detect that GlialCAM changes ClC-2 protein levels (data not shown) and ClC-2 surface expression after transfection of HeLa cells or transduction of primary astrocytes, as ascertained in a chemiluminescence assay (Figure S3).

Since GlialCAM has been described to target MLC1 to cell-cell junctions (López-Hernández et al., 2011b), we assayed if GlialCAM could also modify ClC-2 localization in the same manner. In HeLa cells, ClC-2 transfected alone was detected at the plasma membrane and intracellularly (Figure 3A). Coexpression with GlialCAM directed the ClC-2 channel to cell-cell contacts (Figures 3B–3D), where both proteins colocalized (data not shown). Localization of ClC-2 together with GlialCAM was observed in long (Figure 3B) or short (Figure 3C) cell-cell contact processes and in extensive contact areas between opposite cells (Figure 3D). Such a clustering was never observed in contacting cells expressing only ClC-2 (Figure 3A). Similar results were observed in HEK293 cells (data not shown). We performed analogous experiments in primary cultures of astrocytes, where both proteins are endogenously expressed. In these cultures, adenoviral-mediated expression of ClC-2 with or without GlialCAM showed that the latter protein was necessary to target ClC-2 to astrocyte-astrocyte processes (compare Figures 3E and 3F). In these junctions, ClC-2 and GlialCAM displayed colocalization (Figures 3F–3H).

GlialCAM Modifies ClC-2 Currents

We next asked whether GlialCAM could modify ClC-2 function. Coexpression of GlialCAM and ClC-2 in *Xenopus* oocytes dramatically increased ClC-2-mediated currents and changed their characteristics (Figure 4A). Initial currents measured at +60 mV were more than 15-fold larger in cells coexpressing ClC-2 and GlialCAM compared to ClC-2 alone. Whereas ClC-2 currents are strongly inwardly rectifying and activate slowly upon hyperpolarization, ClC-2/GlialCAM currents were almost ohmic and displayed time-independent, instantaneously active currents (Figure 4B). Of note, the apparent inactivation observed sometimes at very negative voltages is an artifact caused by chloride depletion inside the oocytes.

Similar effects of GlialCAM on ClC-2 currents were seen in transfected HEK293 cells, although a residual time-dependent component was present (Figure 4C). Importantly, GlialCAM alone does not induce any significant current in HEK cells or *Xenopus* oocytes (Figure S4). Similarly, in transfected cells, ClC-2 steady state currents at +60 mV were dramatically increased by GlialCAM (Figure 4D). Specificity of the currents was demonstrated by the characteristic block by extracellular

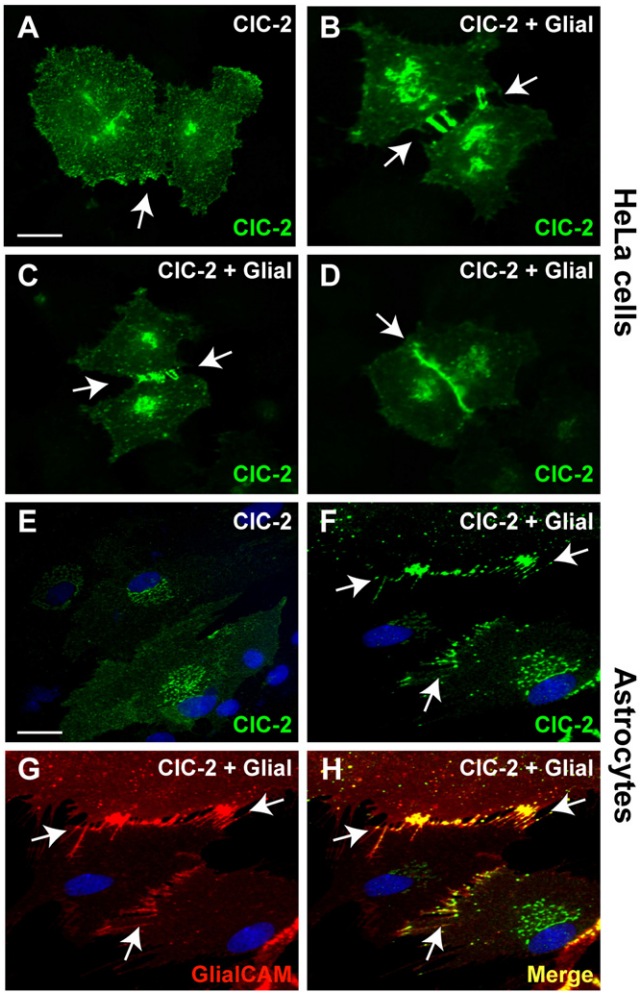

Figure 3. GlialCAM Changes the Subcellular Distribution of ClC-2 in HeLa Cells and in Primary Cultures of Astrocytes

(A–D) GlialCAM changed the subcellular distribution of ClC-2 in transiently transfected HeLa cells from being at the plasma membrane when transfected alone (A) versus being at long cell-cell contact processes (B), at short cell-cell contact processes (C), or in extensive contact regions (D) when cotransfected with GlialCAM (arrows label cell-cell contacts). Scale bar: 10 μm.

(E–H) Astrocytes were transduced with adenoviruses expressing ClC-2 alone or together with C terminally tagged GlialCAM at MOI 3. GlialCAM similarly brought ClC-2 to cell-cell contacts. Arrows point to astrocyte-astrocyte contacts. Immunofluorescence used a flag monoclonal antibody detecting GlialCAM protein (red) or a rabbit polyclonal antibody (C1) detecting ClC-2 (green). Colocalization between the red and the green fluorescence results in a yellow coloring (Merge). Nuclei of astrocytes were stained using DAPI (blue). Scale bar: 20 μm.

See also Figure S3.

iodide (Gründer et al., 1992; Thiemann et al., 1992; Figure 4B) and cadmium (Clark et al., 1998) (data not shown).

To test if GlialCAM may alter native ClC-2 currents we performed whole-cell patch-clamp experiments in differentiated rat astrocytes. These cells exhibit typical hyperpolarization-activated ClC-2-like currents that were blocked by iodide (Ferroni et al., 1997; Makara et al., 2003; Figure 4E). After GlialCAM overexpression, currents were increased and showed a large instantaneous component and less rectification (Figure 4F), qualitatively similar to the effect on ClC-2 in the heterologous systems. These currents were also blocked by iodide to similar degree (Figure 4E).

Even if GlialCAM and connexins do not overlap significantly (Figures 2F and S4D), it may be hypothesized that GlialCAM expression increases ionic currents by stimulating currents through gap junction proteins. However, overexpression of GlialCAM did not modify expression and localization of connexin 43, the major connexin of astrocytes (Figures S4C and S4E). Furthermore, blocking gap junctions with glycyrrhetinic acid did not influence GlialCAM-induced currents in coupled astrocytes (Figure S4F), which were, however, blocked by iodide which is known to block ClC-2 (Gründer et al., 1992; Thiemann et al., 1992; Figure 4F).

We next addressed whether the effect of GlialCAM was specific to ClC-2. GlialCAM did not change currents of ClC-5 at positive or negative voltages (Figure 5A). We studied if human GlialCAM could interact with the ClC-2 ortholog from *Drosophila melanogaster* (DmClC-2) (Flores et al., 2006), whose genome lacks a GlialCAM ortholog. GlialCAM interacted biochemically and increased currents of DmClC-2 (Figures 5B and 5C), suggesting that GlialCAM evolved to interact with the channel at an interface that is evolutionary conserved among ClC-2 like channels. Additionally, we addressed interaction with the closest homolog of GlialCAM named HepaCAM2. No biochemical and functional interaction was observed between HepaCAM2 and ClC-2 (Figures 5D and 5E). Finally, we asked whether wild-type MLC1 or MLC1 containing MLC-causing mutations could influence ClC-2 or ClC-2/GlialCAM induced current in *Xenopus* oocytes. We did not find any effect on ClC-2 mediated currents (Figure 5F).

Insights into the Molecular Mechanism of ClC-2 Activation by GlialCAM

Currents of *Xenopus* oocytes expressing GlialCAM/ClC-2 resemble those of an N-terminal deletion of ClC-2 (ΔN), in which the osmosensitivity and the voltage-dependence is drastically altered (Gründer et al., 1992). This might suggest that GlialCAM activates ClC-2 by interacting with its N terminus. However, we found that GlialCAM still interacted biochemically with (Figure S5A) and targeted the ΔN mutant to cell-cell contacts (Figure S5B) just like wild-type ClC-2. Moreover, GlialCAM potentiated ΔN currents in transfected HEK293 cells (Figure S5C).

We then compared the functional properties of ClC-2, ΔN and GlialCAM/ClC-2. Hypo-osmolarity increased currents of GlialCAM/ClC-2 and ClC-2, but had no effect on ΔN (Gründer et al., 1992; Figure 6A). All of them have the same anion permeability sequence (Figure 6B), strongly suggesting that GlialCAM has no effect on the open-pore properties of the channel. We also addressed whether GlialCAM could increase the single channel conductance of the channel by performing nonstationary noise analysis of currents induced by ClC-2 or by ClC-2/GlialCAM at −100 mV in transfected HEK cells. The conductance of ClC-2 was estimated at 2.9 ± 0.4 pS (n = 8), a value very similar to what has been previously reported (Weinreich and Jentsch,

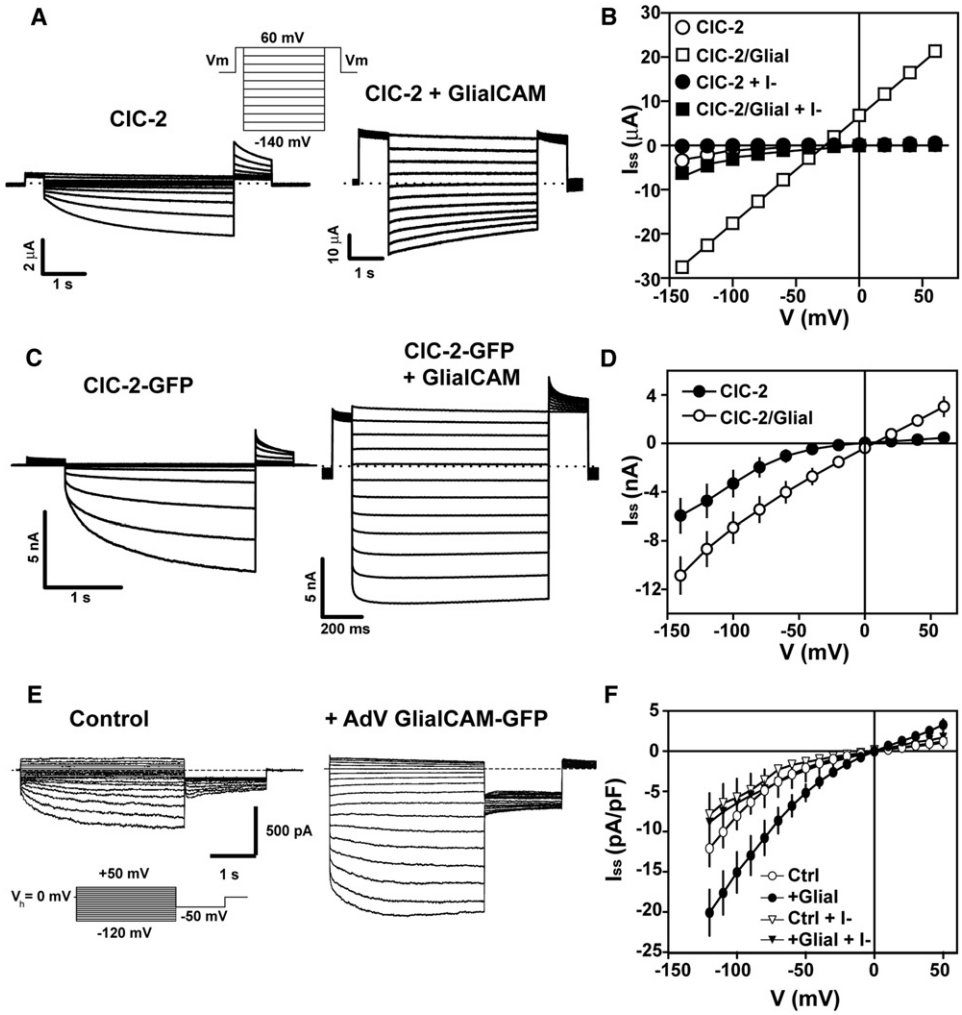

Figure 4. GlialCAM Modifies ClC-2 Currents in *Xenopus* Oocytes, HEK Cells, and Primary Rat Astrocytes

(A) Currents mediated by ClC-2 (left) expressed in oocytes and after coexpression of ClC-2 with GlialCAM (right).

(B) Representative steady-state current-voltage relationship of ClC-2 (circles) and ClC-2 coexpressed with GlialCAM (squares) in chloride (open symbols) or iodide (filled symbols). Average initial currents measured at +60 mV were 0.96 ± 0.17 μA (n = 14) for ClC-2 and 17.2 ± 2.2 μA (n = 10) for ClC-2/GlialCAM.

(C) Typical whole-cell currents from transfected HEK293 cells with ClC-2-GFP alone (left) or together with GlialCAM (right). The GFP tag does not affect ClC-2 current properties.

(D) Average steady-state current voltage from ClC-2-GFP (filled circles) or ClC-2-GFP/GlialCAM (circles) transfected HEK293 cells.

(E) Left: representative trace of whole-cell inwardly rectifying chloride currents in dbcAMP-treated cultured neocortical rat astrocytes. These currents, as described (Ferroni et al., 1997), were blocked when chloride was replaced by iodide (F) and were not blocked by tamoxifen (data not shown). Right: representative trace of chloride currents of dbcAMP-treated astrocytes transduced with adenoviruses expressing GlialCAM fused to GFP. The inset shows the voltage protocol used.

(F) Average steady-state current-voltage relationship of dbcAMP-treated astrocytes (circles, n = 14) or transduced with adenoviruses expressing GlialCAM-GFP (filled circles, n = 14) in chloride medium. Recordings were performed in symmetrical chloride concentrations. In some recordings chloride was exchanged by iodide (triangles or filled triangles). At hyperpolarizing voltages iodide block was by 32.7% ± 3.2% for control astrocytes (n = 6) and by 56.8% ± 2.9% for astrocytes transduced with adenoviruses expressing GlialCAM-GFP (n = 8).

See also Figure S4.

2001). For ClC-2/GlialCAM we obtained a value of 2.6 ± 0.2 pS (n = 8), not statistically significantly different from the value for ClC-2 alone ($p > 0.5$). We conclude that GlialCAM does not modify single-channel properties of ClC-2. Interestingly, GlialCAM similarly diminished the inhibition by acidic pH of both ClC-2 and ΔN (Figure 6C). This result suggested that GlialCAM may activate ClC-2 by opening the common gate that acts on both pores of the homodimeric channel, as this gate is sensitive to acidic pH (Niemeyer et al., 2009).

GlialCAM displays a long cytoplasmatic C terminus comprising about 30% of the protein (Favre-Kontula et al., 2008). However, consistent with its poor sequence conservation between species, the deletion of the entire C terminus did not abolish the interaction with ClC-2, its targeting to cell junctions, and the

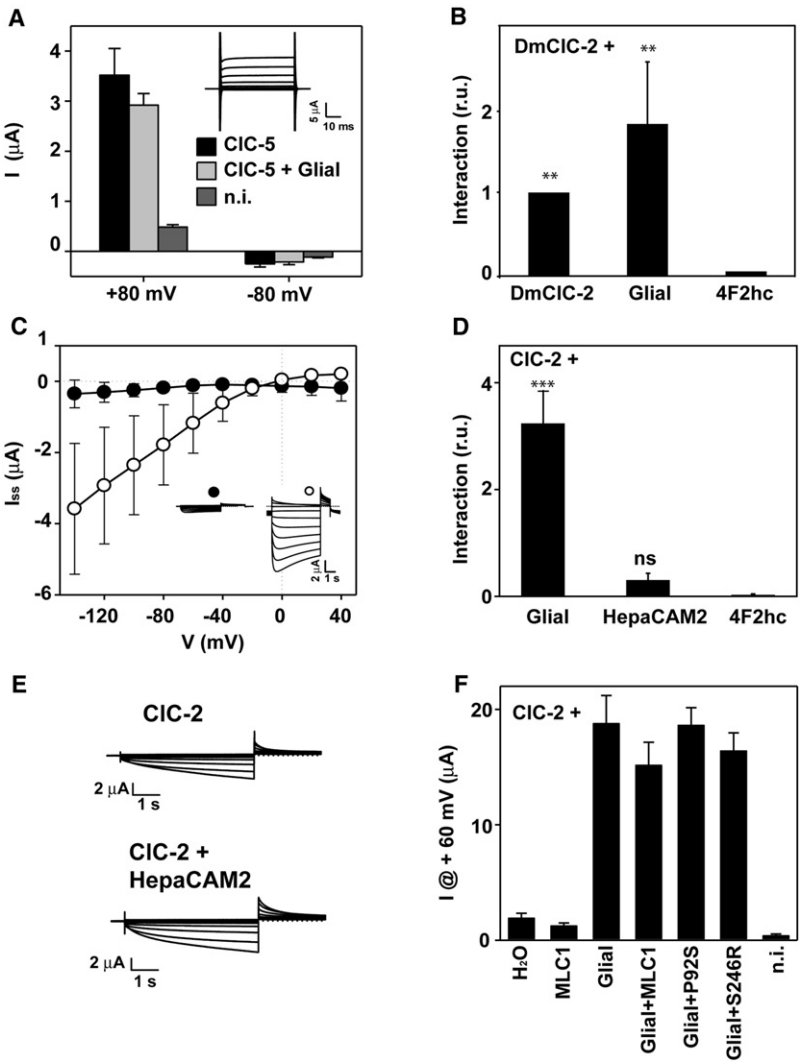

Figure 5. Specificity of the ClC-2 GlialCAM Interaction

(A) Human ClC-5 was expressed in oocytes with and without GlialCAM. Currents were quantified at positive (+80 mV) and negative (−80 mV) voltages 3 days after injection. The inset shows representative ClC-5 + GlialCAM traces using a voltage-clamp protocol with pulses ranging from +120 mV to −120 mV in 20 mV steps.

(B) Interaction between DmClC-2 and DmClC-2 or GlialCAM was monitored using split-TEV assays. 4F2hc was used as a negative control. The result is an average of 5 independent experiments. **$p < 0.01$ versus 4F2hc.

(C) DmClC-2 was expressed in *Xenopus* oocytes by itself or together with GlialCAM. Two days after injection in oocytes DmClC-2 ± GlialCAM currents were determined. Steady state currents are plotted against voltage (n = 5 ± SEM). The inset shows representative current traces of DmClC-2 (filled circle) and DmClC-2 / GlialCAM (open circle).

(D) Interaction between ClC-2 and GlialCAM or HepaCAM2 by split-TEV assays. 4F2hc was used as a negative control. The result is an average of 13 independent experiments. ***$p < 0.001$; "ns" indicates no significant difference versus 4F2hc.

(E) Typical ClC-2 currents in *Xenopus* oocytes expressed by itself (left) or coexpressed with HepaCAM2 (right). HepaCAM2 positive protein expression was assessed by Western blot (data not shown).

(F) Currents measured in *Xenopus* oocytes at + 60 mV after the expression of ClC-2 alone (3 ng), ClC-2 (3 ng) + GlialCAM (5 ng), or ClC-2 (3 ng) + GlialCAM (5 ng) + wild-type MLC1 (3 ng) or containing the MLC-causing mutations P92S and S246R (3 ng). The result is a representative experiment of two experiments with at least 5 oocytes measured for each condition.

activation of ClC-2 currents in transfected cells (Figures S5D–S5F). Hence the interaction between both proteins may depend on the transmembrane and/or the N-terminal part of GlialCAM. Deletion of the N-terminal part of GlialCAM, while keeping the cleavable signal peptide, resulted in a lack of surface expression (data not shown), precluding proper biochemical studies.

Impact of MLC-Related Mutations Identified in *GLIALCAM* on ClC-2

Several *GLIALCAM* mutations found in patients with MLC truncate the protein before the transmembrane domain or result in amino-acid changes in the N-terminal, extracellular part of GlialCAM (López-Hernández et al., 2011a). We studied four of these missense mutations located within the IgV domain (Figure 1A). All GlialCAM proteins containing MLC-causing missense mutations retained their physical interaction with ClC-2 (Figures 7A and S6A) and increased ClC-2 activity similar to wild-type GlialCAM in *Xenopus* oocytes (Figures 7B and S6B) and in transfected cells (data not shown). In contrast, all of them abolished the targeting of ClC-2 to cell junctions in HeLa or HEK293 cells (Figures 7C and 7D).

We also analyzed the effect of the MLC-causing mutations in GlialCAM on the localization of ClC-2 in primary cultures of rat astrocytes through adenoviral-mediated transduction (Figure 8). Coexpression of ClC-2 with GlialCAM mutant variants resulted in intracellular and cell membrane staining of ClC-2 (Figures 8B–8E), but not the typical wild-type GlialCAM induced localization in cell junctions (Figure 8A).

DISCUSSION

In this work, we have identified GlialCAM as an interaction partner of the ClC-2 chloride channel. As ClC-2 is functional in the absence of GlialCAM, albeit displays different biophysical properties, and since GlialCAM shows a much more restricted expression pattern than ClC-2 (Thiemann et al., 1992), it is clear that GlialCAM is not an obligate β-subunit of ClC-2, but an auxiliary subunit that associates with ClC-2 only in some cell types. MLC1 wild-type or containing MLC-causing mutations, by contrast, does not modify ClC-2 currents neither in the presence nor in the absence of GlialCAM, and biochemical studies indicate that ClC-2 and MLC1 do not interact directly (Duarri

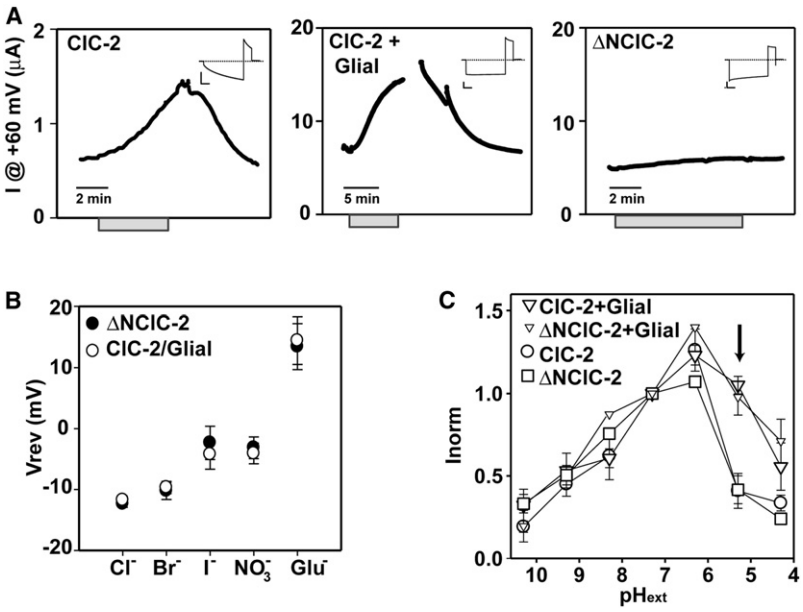

Figure 6. Electrophysiological Characterization of the GlialCAM/ClC-2 Complex

(A) Dependence on the extracellular osmolarity of ClC-2, ClC-2 + GlialCAM, or ΔNClC-2 currents. Gray bars indicate application of the hypotonic solution. Insets show typical responses of the same oocytes to a pulse to −140 mV before swelling.

(B) Reversal potential of ΔNClC-2 (n = 5 ± SEM) and ClC-2/GlialCAM (n = 5 ± SEM) currents under different anionic conditions.

(C) pH dependence of ClC-2 and ΔNClC-2, each without and with GlialCAM. Currents were normalized to the value at pH 7.3. Arrow points to the pH value with the largest difference between the groups that express or not GlialCAM.

See also Figure S5.

et al., 2011). Furthermore, MLC1 expression and localization is unaltered in *Clcn2*$^{-/-}$ mice. These data suggest that GlialCAM/MLC1 and GlialCAM/ClC-2 may form distinct complexes. Recently, the lack of MLC1 has been correlated with a variable impairment in cell volume regulation that may be mediated by the volume regulated anion channel (VRAC) (Ridder et al., 2011). However, VRAC is distinct from ClC-2 as evident from very different biophysical characteristics (Jordt and Jentsch, 1997). Furthermore, the mechanism of modulation of VRAC by MLC1 is unclear. As MLC1 and ClC-2 share GlialCAM as a subunit, we cannot exclude that MLC1 could regulate ClC-2 function in an indirect/unknown manner. Therefore, an interesting hypothesis that should be tested in the next future is whether ClC-2 function is altered in cells lacking MLC1.

GlialCAM by itself localizes to cell-cell junctions (López-Hernández et al., 2011b), probably being retained there by homophilic or heterophilic interactions with membrane proteins of the apposing cell. In other GlialCAM homolog proteins such as the members of the SLAM family (Engel et al., 2003), localization at the immunological synapse of SLAM proteins is achieved by trans-homophilic interactions between the IgV domains of opposite molecules. Furthermore, GlialCAM is also able to localize ClC-2 and MLC1 (López-Hernández et al., 2011b) to cell-cell junctions in heterologous expression systems and in primary cultures of astrocytes. The role of GlialCAM as a ClC-2 subunit appears to be specific within its protein family, as its closest homolog, HepaCAM2, did not interact with ClC-2. GlialCAM carrying MLC-related mutations (López-Hernández et al., 2011a) fails to arrive at cell-cell junctions (López-Hernández et al., 2011b). As a consequence, also their associated subunits, MLC1 and ClC-2, are not properly targeted to cell-cell junctions. Thus, GlialCAM function may be needed to cluster ClC-2 and MLC1 in particular to astrocyte-astrocyte junctions at astrocytic endfeet. Here, the ClC-2 chloride channel may be needed to support a transcellular chloride flux or to compensate large electrochemical ion gradients that may occur at these junctions during ion-driven changes in osmolarity. However, the chloride flux mediated by ClC-2/GlialCAM in cell junctions most likely fulfills a different role compared to the one mediated by gap junctions as these proteins do not colocalize completely. Our experiments also exclude that GlialCAM activates astrocyte gap junctions, since their blockade did not influence currents induced by GlialCAM overexpression, and GlialCAM overexpression had no influence on connexin 43 protein levels or its subcellular localization.

Recent reports indicated that the ClC-2 channel in neurons constitutes a part of the background conductance regulating input resistance and providing an efflux pathway for chloride (Földy et al., 2010; Rinke et al., 2010), which may be a safeguard mechanism to prevent chloride accumulation in active GABAergic synapses. In contrast, the role of ClC-2 in glial cells is unknown. Recordings from mouse slices demonstrated that ClC-2-mediated current was reduced in reactive astrocytes within a lesion (Makara et al., 2003). Strong evidence in favor of an important physiological role of ClC-2 in glial cells is provided by the phenotype of *Clcn2*$^{-/-}$ mice, which display an MLC-like vacuolization in the brain (Blanz et al., 2007). Vacuolization in the brain has been also observed in mice disrupted for the potassium channel Kir4.1 (Neusch et al., 2001) or double-disrupted for connexins 32 *and* 47 (Menichella et al., 2006). These proteins are thought to be crucial for potassium siphoning by glial cells, a process that is needed to avoid neuronal depolarization by extracellular K^+ during repetitive action potential firing (Rash, 2010). In agreement with this role in ion siphoning, in Kir4.1 knockout mice there was no vacuolation in the optic nerve after blocking action potential generation with tetrodotoxin (Neusch et al., 2001). It was neither observed in the *Clcn2*$^{-/-}$ mice possibly because they are blind due to retinal degeneration (Blanz et al., 2007). Hence degeneration in both mouse models depend on nerve activity, in accord with the siphoning process that is required after neuronal repolarization. It has been suggested that ClC-2 may play a role in charge compensation during potassium influx or efflux in glial cells (Blanz et al., 2007).

ClC-2-mediated currents were increased upon GlialCAM expression and showed less inward rectification. However,

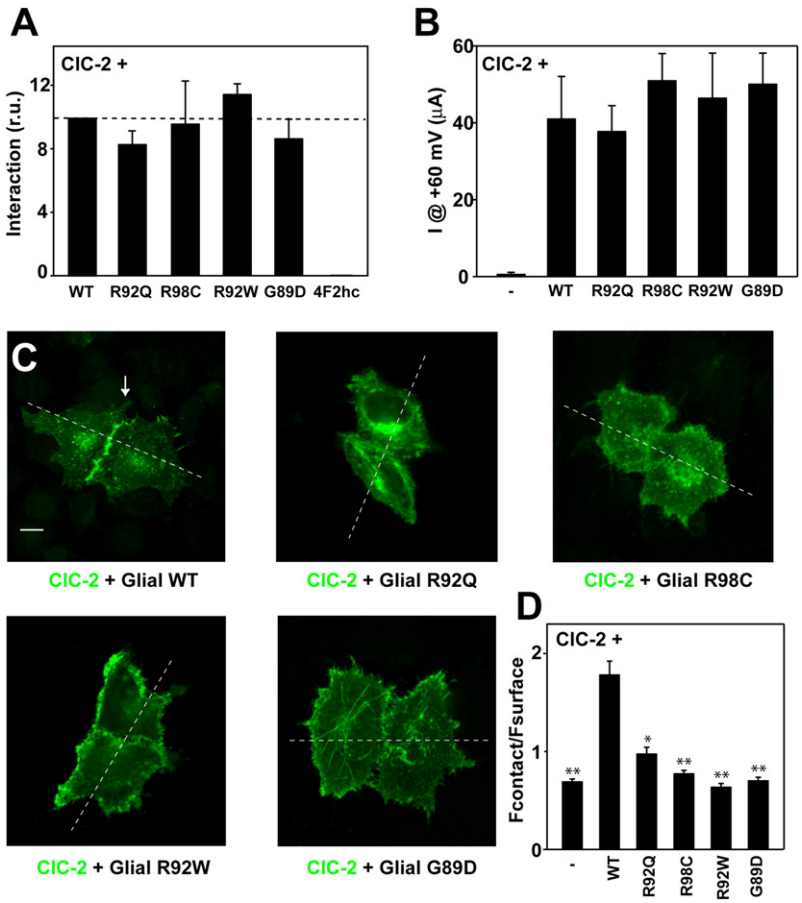

Figure 7. Biochemical and Functional Consequences of *GLIALCAM* Mutations on ClC-2

(A) Interaction between ClC-2 and GlialCAM or GlialCAM containing MLC-related mutations revealed by split-TEV interaction assays (n = 5).

(B) Average instantaneous currents at +60 mV from ClC-2 expressing oocytes coinjected with saturating concentrations of GlialCAM or the indicated GlialCAM variants. The result is an average of n = 5 in each experiment from three independent experiments.

(C) Immunofluorescence of HeLa cells expressing ClC-2 plus wild-type GlialCAM or GlialCAM containing the MLC-related mutations R92Q, R98C, R92W, and G89D. Scale bar: 10 μm. Expression at contact sites and non-contact surface membrane was determined by the analysis of the intensity profile along the dashed line.

(D) Relative fluorescence intensity at cell contacts. Intensity profile analysis revealed that ClC-2 alone had a ratio R of fluorescence $F_{contact}/F_{surface}$ (see Experimental Procedures) of 0.7 ± 0.03 (n = 58), ClC-2 + GlialCAM a value of 1.8 ± 0.14 (n = 55), and the GlialCAM variants studied (with at least 24 pair of cells analyzed) had R values less than 1 (see Experimental Procedures), indicating that the variants containing MLC-related mutations were not able to cluster ClC-2 to cell junctions. *p < 0.05, **p < 0.01 versus wild-type GlialCAM plus ClC-2. Similar results were observed in HEK cells (not shown).

See also Figure S6.

ClC-2 activity recorded in cultured astrocytes (Ferroni et al., 1997) or in astrocytes in brain slices (Makara et al., 2003) resembles that of ClC-2 alone. This may be due to different recording conditions, or, alternatively, it may be that GlialCAM interacts with ClC-2 only under special circumstances, such as those occurring during high neuronal activity.

A polarized distribution of the Kir4.1 channel in astrocyte membranes in contact with endothelial cells, mediated by interaction with proteins of the DGC (dystrophin-glycoprotein complex) (Nagelhus et al., 2004), is required for potassium siphoning. In an analogous way, the polarized localization of ClC-2 mediated by GlialCAM in astrocyte-astrocyte or oligodendrocyte-astrocyte contacts may be also needed to support a directional flux of potassium from neurons to blood vessels. As a cell-adhesion molecule, GlialCAM could influence the expression of other molecules expressed in cell junctions such as connexins. Similar to DGC proteins, the localization in cell-cell contacts of GlialCAM itself and of associated molecules may be achieved by transmediated interactions or by interactions with intracellular scaffolds in each cell. It seems possible that GlialCAM may organize a more extensive cluster of proteins at the astrocytic junctions in the endfeet.

We propose that the lack of the stimulatory effect of GlialCAM on ClC-2 currents, or a mislocalization of this Cl^- channel, or both, will impair glial chloride transport. This may impair not only chloride homeostasis, but also potassium siphoning and cell volume regulation that is particularly important during neuronal activity. This in turn may entail accumulation of osmotically driven water, lead to the vacuolization observed in MLC patients with mutations in *GLIALCAM* or in *Clcn2*$^{-/-}$ mice. Vacuolization observed in MLC patients with *GLIALCAM* mutations could also be due to defects in GlialCAM by itself, or to a mislocalization of MLC1, an established causal player in MLC. Additionally, the adhesive properties of GlialCAM, and their importance for the anatomy of the brain and the pathogenesis of MLC remain to be studied.

The fact that so far no disease-causing *CLCN2* mutation has been found in patients with MLC (Blanz et al., 2007; Scheper et al., 2010) might be explained by the presence of additional symptoms (e.g., blindness, male infertility, as expected from the phenotype of *Clcn2*$^{-/-}$ mice [Bösl et al., 2001]) that could result in improper disease classification. The male infertility could also lead to an underrepresentation of *CLCN2* mutations in the human population. Thus, proof of the involvement of ClC-2 in MLC disease will require, for example, immunolocalization studies in brain biopsies of MLC patients with *GLIALCAM* mutations.

In summary, the discovery of GlialCAM as the first auxiliary subunit of ClC-2 increases the complexity of regulation of the CLC chloride transporter/channel family for which so far only two β-subunits have been described (Estévez et al., 2001; Lange et al., 2006). Our work provides new clues to uncover the physiological role of the ClC-2 channel in glial cells, and suggests that

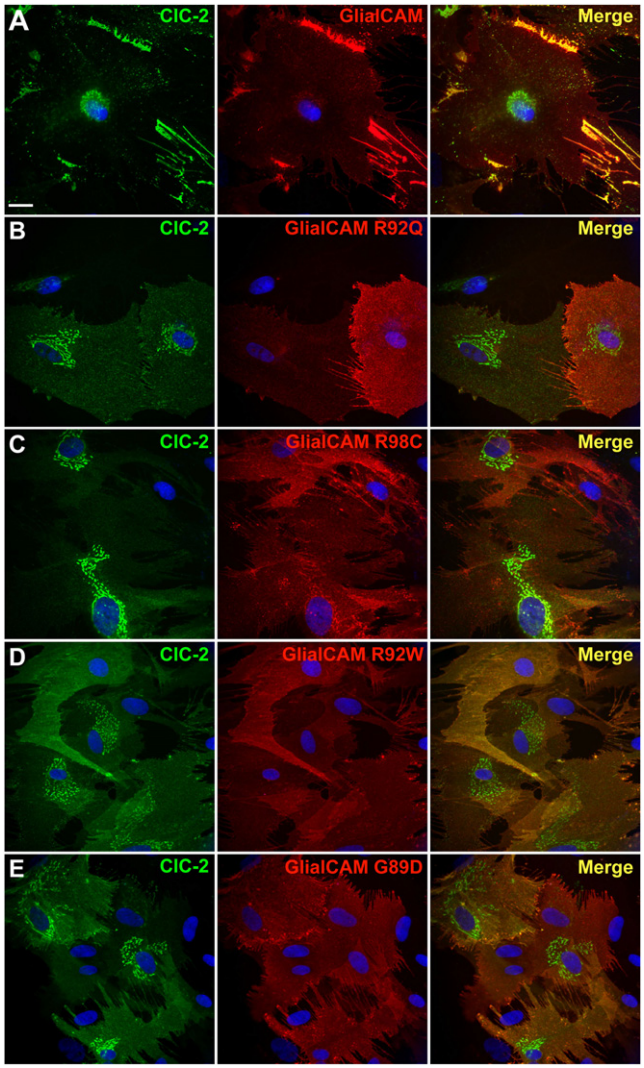

Figure 8. ClC-2 and GlialCAM Subcellular Localization Changes Caused by *GLIALCAM* Mutations in Primary Cultures of Astrocytes

(A–E) Astrocytes were cotransduced with adenoviruses expressing ClC-2 together with wild-type GlialCAM (A) or containing the MLC-related mutations R92Q (B), R98C (C), R92W (D), and G89D (E). Cells were fixed, permeabilized, and then immunofluorescence was performed with a rabbit polyclonal antibody against ClC-2 (green) and a monoclonal antibody detecting GlialCAM protein (red). Nuclei were stained with DAPI (blue). Colocalization between the green and the red channel is shown in yellow. Images correspond to representative cells from three independent experiments. Scale bar: 20 μm.

the ClC-2 channel may be involved in the physiopathology of MLC disease.

EXPERIMENTAL PROCEDURES

Biochemistry

Proteomic analysis: for solubilization, membrane vesicles (1 mg) were resuspended in ComplexioLyte buffer 47a (at 0.8 mg protein/ml, LOGOPHARM GmbH, Germany; with protease inhibitors), incubated for 30 min at 4°C and cleared by ultracentrifugation (10 min at 150,000 × g). 0.8 ml solubilizates were incubated for 2 hr at 4°C with 10 μg of immobilized anti-rabbit GlialCAM (López-Hernández et al., 2011a), anti-mouse GlialCAM (Vitro, Spain) and control IgG (Upstate, USA), respectively. After brief washing (2 × 5 min) with ComplexioLyte 47a, bound proteins were eluted with Laemmli buffer (DTT added after elution). Eluates were shortly run on SDS-PAGE gels and silver-stained prior to tryptic digestion for MS analysis. LC-MS/MS analysis was performed as described (López-Hernández et al., 2011a). Immunoprecipitation and western blot studies of HeLa cells transiently transfected or solubilized rat brain to confirm protein-protein interactions with ClC-2 and GlialCAM antibodies was performed as described (López-Hernández et al., 2011a). Relative MS sequence coverage of ClC-2 protein (Figure S1) was calculated as $SC = N_i/(N_i + N_{an})$, where N_i is the number of amino acid residues of the identified peptides (with Mascot score $\geq$ 20) and N_{an} is the number of MS-accessible but not identified amino acids (peptides with mass of 740–3,000 u) of the respective Swiss-Prot sequence.

Molecular Biology

Rat ClC-2 and the N-terminal deletion (Δ16–61) mutant ΔN (Gründer et al., 1992) constructs for expression in oocytes were in the pTLN vector (Lorenz et al., 1996). For localization studies in HEK293 or HeLa cells, rClC-2 and ΔN were C-terminally fused to GFP or to flag. DmClC-2 and ClC-2 with an HA extracellular tag was provided by LP Cid (Centro de Estudios Científicos, Chile). GlialCAM-ΔC was constructed eliminating residues from 289 until the stop codon.

Voltage-Clamp Experiments

Xenopus oocytes were injected and maintained as described (Estévez et al., 2003). For ClC-2, 5 ng cRNA and for ΔN 0.25 ng cRNA/oocyte were injected. When coexpressing, 1.25 ng cRNA of GlialCAM were coinjected with ClC-2. Oocytes were perfused with (in mM): 100 NaCl, 5 $MgSO_4$, and 10 HEPES/NaOH (pH 7.3). To estimate the specific ClC-2-mediated chloride currents, iodide (100 mM NaI replacing the NaCl), which blocks ClC-2-mediated outward currents (Gründer et al., 1992; Thiemann et al., 1992), was applied in every experiment. Oocytes which did not exhibit a significant block were discarded. For selectivity experiments (Figure 6B), 100 mM Cl^- was exchanged by 100 mM of the tested anion. For pH experiments, 10 mM buffer was used (pH 10–9: CAPS [*N*-cyclohexyl-3-aminopropanesulfonic acid]; pH 8–7: HEPES; pH 6–5: MES; and pH 4: Glutamic acid). Hypotonicity effects were studied as described (Gründer et al., 1992). For ClC-2, an initial 1 s voltage pulse at +60 mV was applied, followed by 5 s voltage steps from −140 mV to +60 mV in 20 mV increments and a tail pulse of 1 s to 60 mV. To quantify expression levels, the initial tail current (at +60 mV) after the −140 mV test pulse was estimated by back extrapolation of a single exponential fit to the decaying tail current. To estimate the number of constitutively active channels, instantaneous currents were measured during a short test pulse to +60 mV without prior activation by hyperpolarization.

Patch-Clamp Experiments

Fluorescent HEK293 cells, expressing CLC-2-GFP or ΔN-GFP with or without GlialCAM, were measured with an extracellular solution containing (in mM): 140 NaCl, 2 $MgSO_4$, 2 $CaCl_2$, and 10 HEPES/NaOH (pH 7.3) using standard patch-clamp technique. Intracellular solution was (in mM) 130 NaCl, 2 $MgSO_4$, 2 EGTA, and 10 HEPES/NaOH (pH 7.3). Only cells for which currents were reversibly blocked by iodide were used for analysis. Patch-clamp of astrocytes was performed as described (Ferroni et al., 1997).

Surface Expression by Chemiluminescence

Surface expression in transfected mammalian cells or astrocytes was performed similarly as previously described (Duarri et al., 2008; Teijido et al., 2004). Briefly, 48 hr after transfection, cells were cleaned with PBS and fixed with 3% paraformaldehyde. After PBS washing, cells were blocked with 1% BSA in PBS for 30 min, and incubated with 1 ml of 3F10 anti-HA antibody at 0.2 μg/ml in blocking solution for 1 hr at RT. Cells were washed six times with blocking solution, and incubated for 20 min with 1 ml of a 1:1,000 dilution horseradish peroxidase-coupled secondary antibody (donkey anti-rat IgG, Jackson, Suffolk, UK) in blocking solution. Cells were washed four times with blocking solution and eight times with PBS. Luminescence was measured

of one dish at a time with 500 μl of Power Signal ELISA solution (Pierce) in a Turner TD-20/20 luminometer (Turner Biosystems, Madison, WI, USA).

Immunological Procedures

Two immune sera against ClC-2 were generated against overlapping sequences of the C terminus. In the first antibody (C1 Ab), the peptide used for immunization was (C)HGLPREGTPSDSDDKSQ. The native protein sequence contains a cysteine residue instead of the highlighted serine in order to avoid coupling this residue to the carrier protein. In the second antibody (C2 Ab), the peptide used for immunization was (C)RSRHGLPREGTPSDSDD. (C) is the cysteine that was used for coupling. Affinity purification of the antibodies was used as described (López-Hernández et al., 2011a). Mostly, the C1 antibody was used in western blot studies, and the C2 antibody was used in immunoprecipitation, immunocytochemistry, and EM immunogold. Both antibodies gave no staining in the *Clcn2*$^{-/-}$ mice.

Primary Culture and Adenoviral Transduction

Rat primary quiescent astrocyte cultures were prepared as described previously (Duarri et al., 2008). Dibutyryl-cAMP differentiated rat astrocytes were obtained as described (Ferroni et al., 1997). Adenoviruses expressing three copies of the flag epitope fused to human GlialCAM, either wild-type or containing mutations have been described (López-Hernández et al., 2011a). Adenoviruses expressing GlialCAM fused to EmGFP or ClC-2 fused to three copies of the Flag epitope or containing an extracellular HA epitope were constructed in a similar manner. Transduction of astrocytes was performed as already described (López-Hernández et al., 2011a).

Immunofluorescence and Electron Microscopic Studies

Tissue immunohistochemistry and immunofluorescence were performed as previously described (Blanz et al., 2007; Teijido et al., 2004). For electron microscopic studies, human cerebellum samples were processed as previously described (López-Hernández et al., 2011a).

Quantification of Localization in Cell Contacts

Image J (http://rsbweb.nih.gov/ij/) was used to quantify fluorescence at cell contacts and in the plasma membrane at cell contact free sites by performing intensity profile experiments. We defined a ratio (R) considering the fluorescence signal at the plasma membrane of two cells (cell 1 and cell 2) and the signal in junctions. [$R = F_{junction}/(F_{membrane1}+F_{membrane2})$]. Thus, if the R value is > 1, the signal will be concentrated at junctions.

Split-TEV Method

Split-TEV (Tobacco etch virus protease) assays were performed as described (López-Hernández et al., 2011b). We used a mutant form of the TEV protease (S219V) which prevents its self-digestion but does not affect its catalytic efficiency. The oligopeptide substrate used as the TEV protease-recognition site was ENLYFQS, and the chimeric transcription factor used was GV (obtained from the pM3-VP16 vector) (Clontech, Nucliber, Madrid, Spain), which contains the yeast Gal4DNA binding domain and the herpes simples VP16 transactivaction domain. After TEV protease cleavage, GV translocates into the nucleus and induces the reporter Gaussia Luciferase gene expression (pNEBr-X1Gluc) (New England BioLabs, IZASA, Barcelona, Spain), which is secreted into the cell culture medium.

TEV protease was divided in two fragments: the TEV-N (residues 1–118) and the TEV-C (residues 119–242). We fused the TEV-N fragment, the TEV protease recognition site and the chimeric transcription factor GV to the C-terminal of ClC-2, the mutant ΔNClC-2, or DmClC-2 in a pCDNA3 vector containing a CMV promoter. In addition, we fused the TEV-C fragment to the C-terminal of ClC-2, ClC-5, ΔNClC-2, GlialCAM wild-type, HepaCAM2, GlialCAMΔC, GlialCAM containing the mutations R92Q, R98C, R92W, and G89D, and the adenosine 2A receptor. The fusion of the TEV-C fragment to 4F2hc was done N-terminal. All the proteins with the TEV-C fragments were cloned in a pCDNA6.2/V5-pL Dest, containing the herpes simplex virus thymidine kinase (HSV-TK) promoter, to provide low to moderate levels of expression.

All the expression plasmids were constructed by PCR using a polymerase with proofreading (KOD Hot Start polymerase, Calbiochem, Darnstadt, Germany), adding the attB1, attB2, attB5R, or attB5 recombination sites compatible with the Multisite Gateway System (Invitrogen, Carlsbad, CA, USA). All protocols were performed according to the manufacturer's instructions (Invitrogen).

HeLa cells were transiently transfected with the corresponding cDNA constructs. The total DNA transfected was 2 μg, with the following ratios: 0.75 μg of each protein containing the TEV-N and the TEV-C fragments, 0.3 μg of the reporter gene pNEBr-X1GLuc, and 0.2 μg of the pCMV-βGal vector, which was used to monitor the transfection efficiency. After 48 hr, 20 μl were removed from the supernatant of the cells and Gaussia luciferase activity was measured in a TD-20/20 luminometer (Turner BioSystems, Madison, USA), after the addition of 20 μM of native colenterazine. To normalize the data, cells were solubilized and 30 μl of the cell lysates were used to measure the β-Galactosidase enzyme activity using the Luminiscent β-Galactosidase Detection Kit II (Clontech) in the same luminometer.

Statistical Analyses

For determination of the statistical significance between groups, either the Student's t test or the Bonferroni's comparison test were used. p values are annotated in each figure. Values depicted are means ± SEM.

SUPPLEMENTAL INFORMATION

Supplemental Information includes six figures and can be found with this article online at doi:10.1016/j.neuron.2011.12.039.

ACKNOWLEDGMENTS

We thank Pablo Cid for the gift of DmClC-2 and human ClC-2 with an HA extracellular tag, Muriel Auberson for the generation of the ClC-2 C1 antibody and Soledad Alcántara for the NG2 antibody. We thank Alejandro Barrallo and Manuel Palacín for comments on the manuscript. This study was supported in part by SAF 2009-07014 (R.E.), PS09/02672-ERARE to R.E., ELA Foundation 2009-017C4 project (R.E. and V.N.), 2009 SGR 719 to R.E., SAF 2009-12606-C02-02 (V.N.), 2009 SGR01490 to V.N., FIS08/0014 (X.G.), FIS PI11/01601 (X.G.), and 2009 SGR869 (X.G.). R.E. is a recipient of an ICREA Academia prize. M.P. and E.J. are supported by the Compagnia San Paolo (Torino, Italy), Telethon Italy (GGP08064), and the Italian Institute of Technology (progetto SEED). This work is dedicated to the memory of Günter Jeworutzki.

Accepted: December 23, 2011
Published: March 7, 2012

REFERENCES

Blanz, J., Schweizer, M., Auberson, M., Maier, H., Muenscher, A., Hübner, C.A., and Jentsch, T.J. (2007). Leukoencephalopathy upon disruption of the chloride channel ClC-2. J. Neurosci. *27*, 6581–6589.

Bösl, M.R., Stein, V., Hübner, C., Zdebik, A.A., Jordt, S.E., Mukhopadhyay, A.K., Davidoff, M.S., Holstein, A.F., and Jentsch, T.J. (2001). Male germ cells and photoreceptors, both dependent on close cell-cell interactions, degenerate upon ClC-2 Cl^- channel disruption. EMBO J. *20*, 1289–1299.

Brignone, M.S., Lanciotti, A., Macioce, P., Macchia, G., Gaetani, M., Aloisi, F., Petrucci, T.C., and Ambrosini, E. (2011). The beta1 subunit of the Na,K-ATPase pump interacts with megalencephalic leucoencephalopathy with subcortical cysts protein 1 (MLC1) in brain astrocytes: new insights into MLC pathogenesis. Hum. Mol. Genet. *20*, 90–103.

Clark, S., Jordt, S.E., Jentsch, T.J., and Mathie, A. (1998). Characterization of the hyperpolarization-activated chloride current in dissociated rat sympathetic neurons. J. Physiol. *506*, 665–678.

Duarri, A., Teijido, O., López-Hernández, T., Scheper, G.C., Barriere, H., Boor, I., Aguado, F., Zorzano, A., Palacín, M., Martínez, A., et al. (2008). Molecular pathogenesis of megalencephalic leukoencephalopathy with subcortical cysts: mutations in MLC1 cause folding defects. Hum. Mol. Genet. *17*, 3728–3739.

Duarri, A., Lopez de Heredia, M., Capdevila-Nortes, X., Ridder, M.C., Montolio, M., López-Hernández, T., Boor, I., Lien, C.F., Hagemann, T., Messing, A., et al. (2011). Knockdown of MLC1 in primary astrocytes causes cell vacuolation: a MLC disease cell model. Neurobiol. Dis. *43*, 228–238.

Engel, P., Eck, M.J., and Terhorst, C. (2003). The SAP and SLAM families in immune responses and X-linked lymphoproliferative disease. Nat. Rev. Immunol. *3*, 813–821.

Estévez, R., Boettger, T., Stein, V., Birkenhäger, R., Otto, E., Hildebrandt, F., and Jentsch, T.J. (2001). Barttin is a Cl^- channel beta-subunit crucial for renal Cl^- reabsorption and inner ear K^+ secretion. Nature *414*, 558–561.

Estévez, R., Schroeder, B.C., Accardi, A., Jentsch, T.J., and Pusch, M. (2003). Conservation of chloride channel structure revealed by an inhibitor binding site in ClC-1. Neuron *38*, 47–59.

Fava, M., Ferroni, S., and Nobile, M. (2001). Osmosensitivity of an inwardly rectifying chloride current revealed by whole-cell and perforated-patch recordings in cultured rat cortical astrocytes. FEBS Lett. *492*, 78–83.

Favre-Kontula, L., Rolland, A., Bernasconi, L., Karmirantzou, M., Power, C., Antonsson, B., and Boschert, U. (2008). GlialCAM, an immunoglobulin-like cell adhesion molecule is expressed in glial cells of the central nervous system. Glia *56*, 633–645.

Ferroni, S., Marchini, C., Nobile, M., and Rapisarda, C. (1997). Characterization of an inwardly rectifying chloride conductance expressed by cultured rat cortical astrocytes. Glia *21*, 217–227.

Flores, C.A., Niemeyer, M.I., Sepúlveda, F.V., and Cid, L.P. (2006). Two splice variants derived from a Drosophila melanogaster candidate ClC gene generate ClC-2-type Cl^- channels. Mol. Membr. Biol. *23*, 149–156.

Földy, C., Lee, S.H., Morgan, R.J., and Soltesz, I. (2010). Regulation of fast-spiking basket cell synapses by the chloride channel ClC-2. Nat. Neurosci. *13*, 1047–1049.

Gründer, S., Thiemann, A., Pusch, M., and Jentsch, T.J. (1992). Regions involved in the opening of CIC-2 chloride channel by voltage and cell volume. Nature *360*, 759–762.

Jordt, S.E., and Jentsch, T.J. (1997). Molecular dissection of gating in the ClC-2 chloride channel. EMBO J. *16*, 1582–1592.

Lange, P.F., Wartosch, L., Jentsch, T.J., and Fuhrmann, J.C. (2006). ClC-7 requires Ostm1 as a beta-subunit to support bone resorption and lysosomal function. Nature *440*, 220–223.

Leegwater, P.A., Yuan, B.Q., van der Steen, J., Mulders, J., Könst, A.A., Boor, P.K., Mejaski-Bosnjak, V., van der Maarel, S.M., Frants, R.R., Oudejans, C.B., et al. (2001). Mutations of MLC1 (KIAA0027), encoding a putative membrane protein, cause megalencephalic leukoencephalopathy with subcortical cysts. Am. J. Hum. Genet. *68*, 831–838.

López-Hernández, T., Ridder, M.C., Montolio, M., Capdevila-Nortes, X., Polder, E., Sirisi, S., Duarri, A., Schulte, U., Fakler, B., Nunes, V., et al. (2011a). Mutant GlialCAM causes megalencephalic leukoencephalopathy with subcortical cysts, benign familial macrocephaly, and macrocephaly with retardation and autism. Am. J. Hum. Genet. *88*, 422–432.

López-Hernández, T., Sirisi, S., Capdevila-Nortes, X., Montolio, M., Fernández-Dueñas, V., Scheper, G.C., van der Knaap, M.S., Casquero, P., Ciruela, F., Ferrer, I., et al. (2011b). Molecular mechanisms of MLC1 and GLIALCAM mutations in megalencephalic leukoencephalopathy with subcortical cysts. Hum. Mol. Genet. *20*, 3266–3277.

Lorenz, C., Pusch, M., and Jentsch, T.J. (1996). Heteromultimeric CLC chloride channels with novel properties. Proc. Natl. Acad. Sci. USA *93*, 13362–13366.

Makara, J.K., Rappert, A., Matthias, K., Steinhäuser, C., Spät, A., and Kettenmann, H. (2003). Astrocytes from mouse brain slices express ClC-2-mediated Cl^- currents regulated during development and after injury. Mol. Cell. Neurosci. *23*, 521–530.

Menichella, D.M., Majdan, M., Awatramani, R., Goodenough, D.A., Sirkowski, E., Scherer, S.S., and Paul, D.L. (2006). Genetic and physiological evidence that oligodendrocyte gap junctions contribute to spatial buffering of potassium released during neuronal activity. J. Neurosci. *26*, 10984–10991.

Nagelhus, E.A., Mathiisen, T.M., and Ottersen, O.P. (2004). Aquaporin-4 in the central nervous system: cellular and subcellular distribution and coexpression with KIR4.1. Neuroscience *129*, 905–913.

Neusch, C., Rozengurt, N., Jacobs, R.E., Lester, H.A., and Kofuji, P. (2001). Kir4.1 potassium channel subunit is crucial for oligodendrocyte development and in vivo myelination. J. Neurosci. *21*, 5429–5438.

Niemeyer, M.I., Cid, L.P., Yusef, Y.R., Briones, R., and Sepúlveda, F.V. (2009). Voltage-dependent and -independent titration of specific residues accounts for complex gating of a ClC chloride channel by extracellular protons. J. Physiol. *587*, 1387–1400.

Rash, J.E. (2010). Molecular disruptions of the panglial syncytium block potassium siphoning and axonal saltatory conduction: pertinence to neuromyelitis optica and other demyelinating diseases of the central nervous system. Neuroscience *168*, 982–1008.

Ridder, M.C., Boor, I., Lodder, J.C., Postma, N.L., Capdevila-Nortes, X., Duarri, A., Brussaard, A.B., Estevez, R., Scheper, G.C., Mansvelder, H.D., and van der Knaap, M.S. (2011). Megalencephalic leucoencephalopathy with cysts: defect in chloride currents and cell volume regulation. Brain *134*, 3342–3354.

Rinke, I., Artmann, J., and Stein, V. (2010). ClC-2 voltage-gated channels constitute part of the background conductance and assist chloride extrusion. J. Neurosci. *30*, 4776–4786.

Scheper, G.C., van Berkel, C.G., Leisle, L., de Groot, K.E., Errami, A., Jentsch, T.J., and Van der Knaap, M.S. (2010). Analysis of *CLCN2* as candidate gene for megalencephalic leukoencephalopathy with subcortical cysts. Genet. Test. Mol. Biomarkers *14*, 255–257.

Sík, A., Smith, R.L., and Freund, T.F. (2000). Distribution of chloride channel-2-immunoreactive neuronal and astrocytic processes in the hippocampus. Neuroscience *101*, 51–65.

Teijido, O., Martínez, A., Pusch, M., Zorzano, A., Soriano, E., Del Río, J.A., Palacín, M., and Estévez, R. (2004). Localization and functional analyses of the MLC1 protein involved in megalencephalic leukoencephalopathy with subcortical cysts. Hum. Mol. Genet. *13*, 2581–2594.

Thiemann, A., Gründer, S., Pusch, M., and Jentsch, T.J. (1992). A chloride channel widely expressed in epithelial and non-epithelial cells. Nature *356*, 57–60.

van der Knaap, M.S., Barth, P.G., Stroink, H., van Nieuwenhuizen, O., Arts, W.F., Hoogenraad, F., and Valk, J. (1995a). Leukoencephalopathy with swelling and a discrepantly mild clinical course in eight children. Ann. Neurol. *37*, 324–334.

van der Knaap, M.S., Valk, J., Barth, P.G., Smit, L.M., van Engelen, B.G., and Tortori Donati, P. (1995b). Leukoencephalopathy with swelling in children and adolescents: MRI patterns and differential diagnosis. Neuroradiology *37*, 679–686.

van der Knaap, M.S., Barth, P.G., Vrensen, G.F., and Valk, J. (1996). Histopathology of an infantile-onset spongiform leukoencephalopathy with a discrepantly mild clinical course. Acta Neuropathol. *92*, 206–212.

Weinreich, F., and Jentsch, T.J. (2001). Pores formed by single subunits in mixed dimers of different CLC chloride channels. J. Biol. Chem. *276*, 2347–2353.